Procds. of the 16th Asian Regional Conference on Soil Mechanics and Geotechnical Engineering,
October 14-18, 2019, Taipei, Taiwan

Evaluation of the liquefaction potential index in Busan Eco-Delta city, South Korea

Bahareh Bahari[1], T.H. Kim[1], and W. Hwang[1]

[1] Department of Civil and Environmental Engineering, Korea Maritime and Ocean University, 727 Taejong-ro, Yeongdo-Gu, Busan 49112, South Korea

Keywords: Liquefaction; Factor of safety (FS); Liquefaction potential index (LPI); Liquefaction probability; Pore water pressure

Abstract

Soil liquefaction which is a disastrous phenomenon induced by the earthquake, is widely investigated in many researches in geotechnical engineering. In this study, a SPT-N based investigation is carried out to assess the susceptibility of liquefaction in Eco-Delta city, located in the southwestern part of Busan city in South Korea. Data from 229 sites are analyzed for the earthquake of 7.5 magnitude with a peak horizontal acceleration of 0.2*g* to carry out the liquefaction potential index (LPI) through deterministic method. The liquefaction probability is investigated by the reliability method and the liquefaction hazard maps are generated considering three cases for fines content and plasticity index. The Eco-Delta city is found to be highly vulnerable to liquefaction having 91% of sites with *LPI* values greater than 15. The prediction of liquefaction probability as a function of *LPI* is also investigated and limit bound equations are predicted.

1 INTRODUCTION

Liquefactions and associated ground failures have been widely occurred during numerous devastating earthquakes. It is a common result of ground failure during earthquakes and is directly related to tremendous damage to civil infrastructure. It occurs generally due to rapid loading during seismic events where there is not enough time for dissipation of excess pore-water pressures through natural drainage. Increase in pore-water pressures is the result of rapid loading situation which happens in cyclic softening in fine-grained materials. The increased pore water pressure transforms granular materials from a solid to a liquefied state and that's why the shear strength and stiffness of the soil deposit are reduced. Liquefaction-induced ground failure is influenced by the thickness of non-liquefied and liquefied soil layers. It is mostly observed in loose, saturated, and clean to silty sands (Seed and Idriss, 1971). The soil liquefaction depends on the magnitude of earthquake, intensity and duration of ground motion, the distance from the source of the earthquake, site specific conditions, ground acceleration, type of soil and thickness of the soil deposit, relative density, grain size distribution, fines content, plasticity of fines, degree of saturation, confining pressure, permeability characteristics of soil layer, groundwater table, reduction of effective stress, and shear modulus degradation (Youd and Perkins 1978; Youd et al. 2001).

2 INVESTIGATION OF STUDY AREA

Busan province is located in southeastern part of South Korea as shown in Figure 1. It covers an area of about 770 km^2 having the population of about 3.5 million being the second largest city in South Korea. The city is surrounded by the Ulsan province in the north, the Gyeongsangnam-do province in the west and East Sea in the east and south. The city is 400 ~ 800 meters above the sea level. The study area is the Eco-Delta city having the area of 11.77 km^2, which is located in the southwestern part of the Busan city. The soil of this area is all alluvial deposit. The deposit consists of loose sand (upper sand), thick soft clay (upper clay), sand (lower sand), soft clay (lower clay) and sand and gravel layers on bedrocks that sometimes reaches over 50~60 meters in thickness (Figure 2). Geological investigations imply that the sand layers cover from the ground surface to the depth of about 8 meters in most of the Eco-Delta city and the clay or silt cover over the depth of 12 meters (Lim 2018).

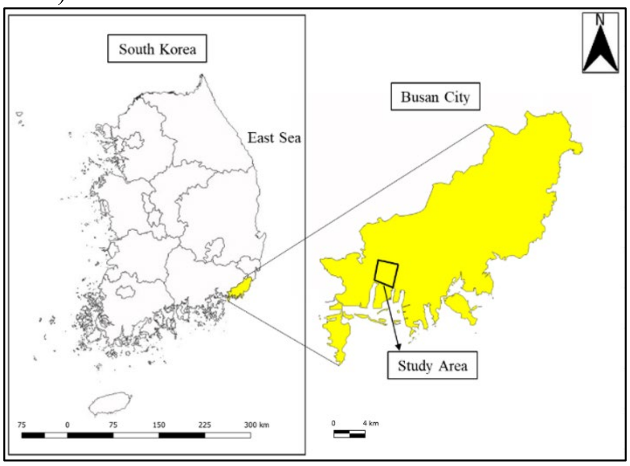

Fig. 1. Location map of the study area

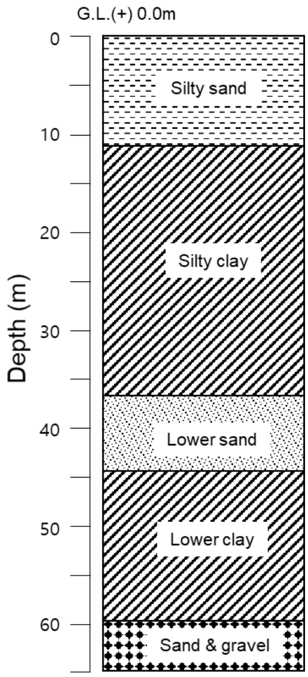

Fig. 2. Representative soil profile

The Sineo mountain, which reaches Yeondae in Gadeok island, surrounds the western part of the city. In the east, there are Geumjeong and Baegyang mountains. The main rivers in the city are Nakdong, Suyeong, Oncheon and Dongcheon. Busan city is the cretaceous Yangsan basin, which is the largest basin in South Korea. It is divided into the nutrient basin, the sedimentary rocks of the Shindong formation, the Hayang formation, and the Bulguksa granite formation. The seismic structure of the city consists of the Korean peninsula which is the largest structure line of the Yangsan fault system extending from north to the northeast direction, the Dongnae fault which passes through the downtown of Busan city, and the small fault of Ilgwang fault [Chough and Sohn, 2010].

Recently South Korea has experienced two earthquakes near the Busan city which were the Gyeonju earthquake in 2016 having the magnitude of 5.8 and the Pohang earthquake in 2017 having the magnitude of 5.4. In order to investigate the critical condition in liquefaction analysis, the earthquake with a magnitude of 7.5 is considered in this study.

3 DETERMINISTIC EVALUATION OF LIQUEFACTION PROBABILITY

The potential for liquefaction to occur at certain depth in a site is quantified as the factor of safety against liquefaction (FS) which is the ratio of cyclic resistance ratio to cyclic stress ratio. There are several in-situ tests to calculate the FS of a soil layer such as standard penetration test (SPT), cone penetration test (CPT), Becker penetration test (BPT) and shear wave velocity (Vs) test (Youd et al., 2001). Among them, SPT-based simplified procedure which was proposed by Seed and Idriss (1971) is widely used to calculate the liquefaction resistance of soils.

The equation for calculation of FS can be defined as Equation (1) [Seed and Idriss, 1971]:

$$FS = \frac{CRR_{7.5}}{CSR} MSF \tag{1}$$

where CSR is the calculated cyclic stress ratio generated by the earthquake; and $CRR_{7.5}$ is the cyclic resistance ratio for the earthquake of 7.5 magnitude. The cyclic stress ratio can be defined as Equation (2):

$$CSR = \frac{\tau_{av}}{\sigma'_{vo}} = 0.65(\frac{a_{max}}{g})(\frac{\sigma_{vo}}{\sigma'_{vo}})r_d \tag{2}$$

where a_{max} is the peak horizontal ground acceleration induced by the earthquake shaking at the ground surface; g is the gravity acceleration; σ_{vo} and σ'_{vo} are the total and effective vertical overburden stress, respectively, at the particular depth below the ground surface; and r_d is the stress reduction factor which depends to the depth.

In order to determine the a_{max} in the study area, the result of Park et al. [2018] research is used. They investigated the distribution of horizontal peak ground acceleration (PGA) during the Gyeonju earthquake in 2016 and determined that the horizontal peak ground acceleration is about 0.2g in Busan province.

LPI is a single-valued parameter to assess liquefaction potential. It is calculated by integrating the FS along the soil column up to 20 meters depth at a site. There is a weighting function used in LPI to have more weight to the layers closer to the ground surface. The LPI proposed by Iwasaki et al. [1978] is expressed as Equation (3):

$$LPI = \int_0^{20} F(z).w(z)dz \tag{3}$$

where z is depth at the midpoint of the soil layer and varies from 0 to 20 meters. The w(z) is the weighting factor and the F(z) is the severity factor.

In order to show the distribution of the liquefaction risks in the city, the liquefaction hazard maps are appropriate which provide the useful information for geotechnical engineers to check the susceptibility of the area against liquefaction and evaluating the seismic safety plans. Liquefaction hazards are categorized based on the LPI values of sites as LPI=0, 0<LPI≤2, 2<LPI≤5, 5<LPI≤15 and LPI>15 according to the proposed range by Sonmez [2003]. The result of in-situ geotechnical tests are collected for total 229 boreholes including 83 boreholes in part 1, 110 boreholes in part 2 and 36 boreholes in part 3. In order to further investigate the effect of fines content to the liquefaction, three different cases are considered for the percent of fines content as 5%, 15% and 35% and plasticity index as 5%, 10% and 20% for each borehole. The details of calculation for a typical borehole are given in Table 1.

Figures 3, 4 and 5 show the contour maps of the study area based on the FS of Seed and Idriss [1971] method for case 1, 2 and 3, respectively which are generated using QGIS program.

Table 1. Soil characteristics of the typical borehole

Depth (m)	USCS	SPT-N	γ (kN/m^3)	σ'_v (kN/m^2)	CSR
1.5	CL	2	16.2	17.92	-
3.0	SM	2	16.2	27.51	0.225
4.5	SM	3	16.3	37.24	0.247
6.0	SM	5	16.5	47.28	0.258
7.5	SM	4	16.4	57.16	0.263
9.0	SM	4	16.4	67.05	0.263
10.5	SM	4	16.4	76.93	0.259
12.0	SM	3	16.3	86.67	0.252
13.5	ML	2	16.2	96.25	-
15.0	ML	2	16.2	105.8	-
16.5	ML	1	16.1	115.3	-
18.0	ML	3	16.3	125.0	-
19.5	CL	0	16.0	134.3	-

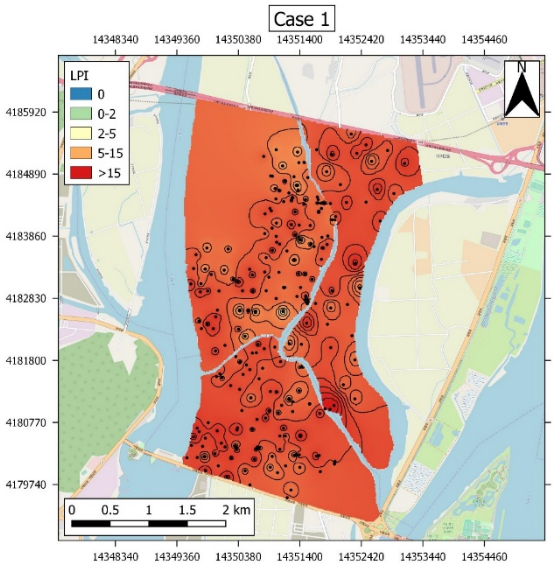

Fig. 3. Liquefaction hazard map based on Seed and Idriss (1971) method for case 1

4 RELIABILITY EVALUATION OF LIQUEFACTION PROBABILITY

Jha and Suzuki [2009] defined a reliability based design safety factor which considers uncertainties in model parameters. Based on this approach, the susceptibility of soil liquefaction is defined in terms of probability of liquefaction. The susceptibility for liquefaction in terms of probability of liquefaction (PL) is obtained from the reliability index β' by Equation (4):

$$P_L = 1 - \Phi(\beta') \quad (4)$$

where $\Phi(.)$ is the standard normal cumulative probability. The reliability index β' can be expressed based on margin of safety approach. Assuming that CSR and CRR follows normal probability distribution, β' is defined as Equation (5) [Hwang et al., 2004]:

$$\beta'_{LN} = \frac{\ln\left[FS\sqrt{\frac{V^2_{CSR_{7.5,\sigma}}+1}{V^2_{CRR_{7.5}}+1}}\right]}{\sqrt{ln\left[(V^2_{CSR_{7.5,\sigma}}+1)(V^2_{CRR_{7.5}}+1)\right]}} \quad (5)$$

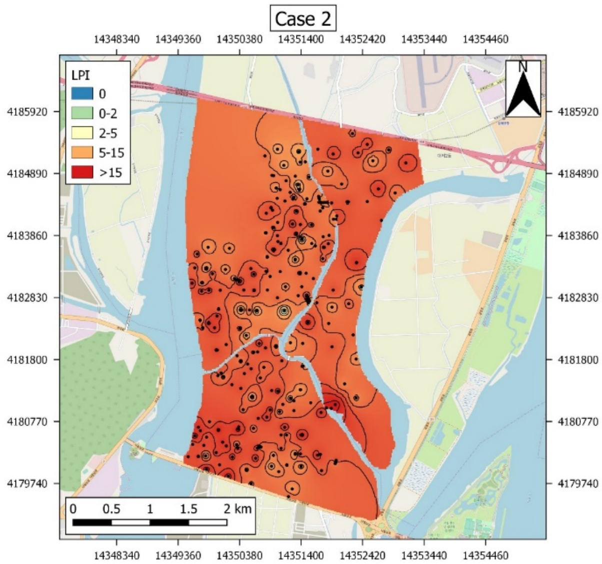

Fig. 4. Liquefaction hazard map based on Seed and Idriss (1971) method for case 2

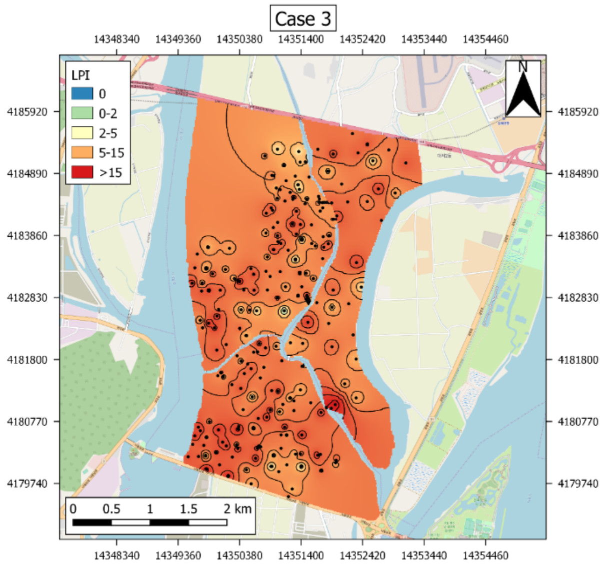

Fig. 5. Liquefaction hazard map based on Seed and Idriss (1971) method for case 3

where V represents the COV (i.e. the ratio of standard deviation to mean) of $CSR_{7.5,\sigma}$ and $CRR_{7.5}$ could be determined by first order second moment (FOSM) method. Using the FOSM method, the COV of $CSR_{7.5,\sigma}$ can be calculated as Equation (6):

$$V^2_{CSR_{7.5,\sigma}} = V^2_{a_{max}} + V^2_{\sigma_v} + V^2_{\sigma'_v} + V^2_{\gamma_d} + V^2_{MSF} + V^2_{k_\sigma} - 2\rho_{\sigma_v\sigma'_v}V_{\sigma'_v}V_{\sigma_v} \quad (6)$$

where V represents the COV and $\rho_{\sigma_v\sigma'_v}$ denotes the correlation coefficient between total and effective stress.

The probability of liquefaction is evaluated as the reliability method and the results for cases 1, 2 and 3 are shown in Figures 6, 7 and 8, respectively.

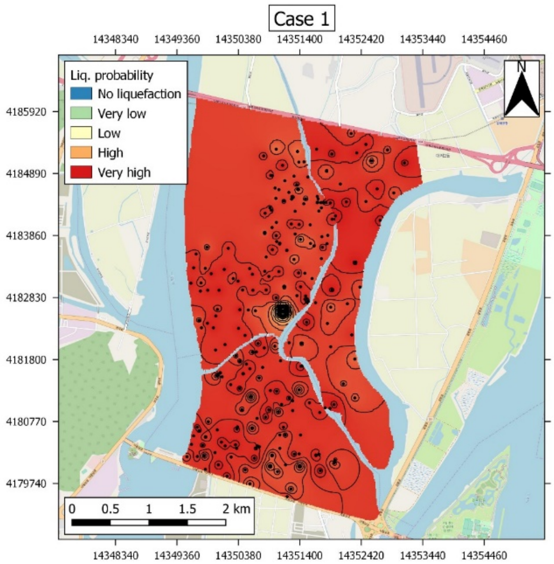

Fig. 6. Liquefaction hazard map based on reliability method for case 1

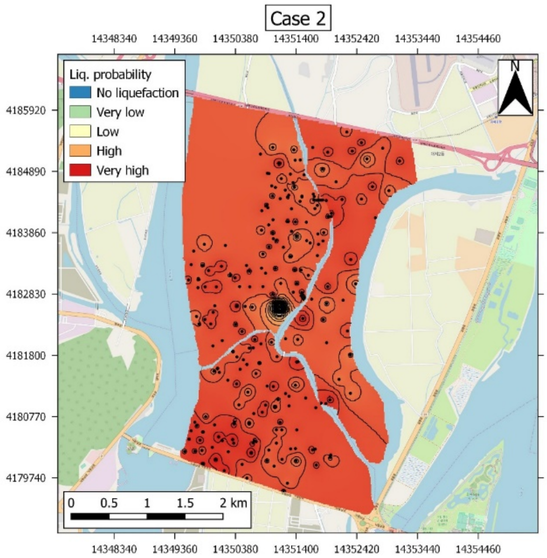

Fig. 7. Liquefaction hazard map based on reliability method for case 2

To compute the probability of liquefaction considering the effect of the depth of liquefiable soil determined from the factor of safety, LPI values are chosen which account the weighting function for the depth. Figure 9 shows the probability of liquefaction as a function of LPI values. This figure shows that the least probability of liquefaction is about 76% that relates to the LPI value of about 2 (red arrow in Figure 9). The probability of liquefaction falls in the area that can be estimated by linear equations which are shown in Figure 9.

5 CONCLUSION

Data from 229 sites are collected and factors of safety against liquefaction are calculated which are used to investigate the LPI. In order to investigate the effect of fines content on liquefaction susceptibility in the study

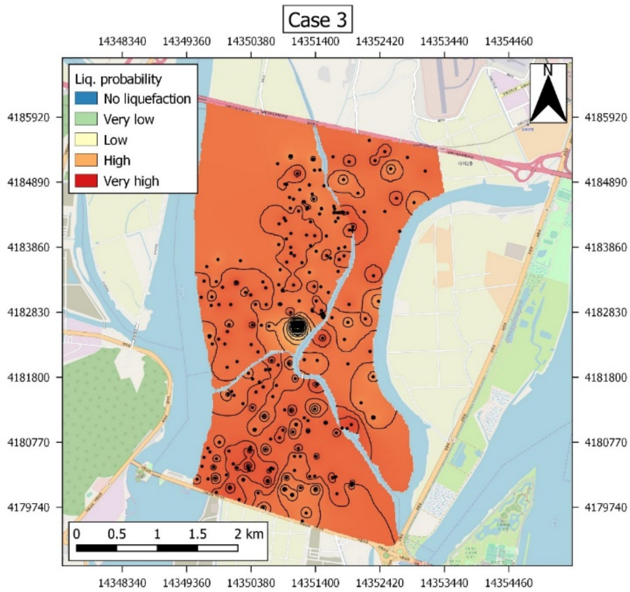

Fig. 8. Liquefaction hazard map based on reliability method for case 3

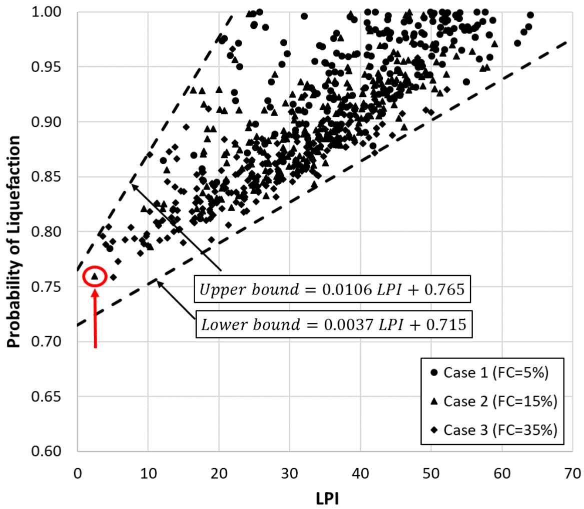

Fig. 9. Relationship between the liquefaction probability and liquefaction potential index

area, three different cases are considered for fines content and plasticity index. The liquefaction probability is also investigated through reliability approach. The liquefaction hazard maps are generated for the area to predict the occurrence of liquefaction for the earthquakes of magnitude 7.5 with peak horizontal ground acceleration of 0.2g. Since the GWT is very high in the study area, and because higher GWT increases the CSR by the ratio of total and effective vertical stress, so it reduces FS against liquefaction and is heavily weighted in computing LPI, and thus, about 91% of the sites showed very high liquefaction susceptibility by LPI values over 15. Moreover, it leads the sites to be unsafe against liquefaction; since only one soil column is safe against liquefaction by the LPI less than 2. So the city is found to be highly vulnerable for liquefaction. Assuming a threshold value of 25% for liquefaction susceptibility, no site is safe against liquefaction through reliability approach. The hazard maps indicate that the susceptibility of liquefaction decreases by increasing the percent of fines content and plasticity index from case 1 to case 2 and from case 2 to case3, as it was expected. The number of sites predicted to be liquefied by reliability approach are higher comparing to the deterministic approach as well as the liquefaction severity.

REFERENCES

Chough, S. K. and Sohn, Y. K. (2010). Tectonic and sedimentary evolution of a cretaceous continental arc-backarc system in the Korean peninsula: New view, Korea Earth Science Reviews 101, 225–249. https://doi.org/10.1016/j.earscirev.2010.05.004.

Hwang, J. H., Yang, C. W. and Juang, D. S. (2004). A practical reliability-based method for assessing soil liquefaction potential, Soil Dynamics and Earthquake Engineering 24, 761–770. https://doi.org/10.1016/j.soildyn.2004.06.008.

Iwasaki, T., Tatsuoka, F., Tokida, K.-I. and Yasuda, S. (1978). A practical method for assessing soil liquefaction potential based on case studies at various sites in Japan, Proc. of second International Conference on Microzonation, San Francisco, pp. 885–896.

Jha, S. K., Suzuki, K. (2009). Liquefaction potential index considering parameter uncertainties, Engineering Geology 107, 55–60. https://doi.org/10.1016/j.enggeo.2009.03.012.

Lim, H. J. (2018). Seismic hazard assessment using geotechnical characteristics and geographic information system in Busan city, M.Sc. Thesis, Civil Engineering Dept., Busan National University, Busan (In Korean with English abstract). http://dcollection.pusan.ac.kr/common/orgView/000000133364.

Park, J. B., Ahn, J. H., Choi, H., Kim, G. S. and Kang, G. C. (2018). Application of existing distance attenuation relationships using PGAs recorded during earthquakes, Journal of the Korean Society of Hazard Mitigation 18(6), 149–159. (in Korean with English abstract). j-kosham.or.kr/upload/pdf/KOSHAM-2018-18-6-149.pdf.

Seed, H. B. and Idriss, I. M. (1971). Simplified procedure for evaluating soil liquefaction potential, Journal of Geotechnical Engineering, ASCE 97(9), 1249–1273.

Sonmez, H. (2003). Modification of the liquefaction potential index and liquefaction susceptibility mapping for a liquefaction-prone area (Inegol, Turkey), Environmental Geology 44(7), 862–871. https://doi.org/10.1007/s00254-003-0831-0.

Youd, T., Perkins, D. M. (1987). Mapping of liquefaction severity index, Journal of Geotechnical Engineering, ASCE 113(11), 1374–1392. https://doi.org/10.1061/(ASCE)0733-9410(1987)113:11(1374).

Youd, T. L., Idriss, I. M., Andrus, R. D., Arango, I., Castro, G., Christian, J. T., Dobry, R., Finn, W. D. L., Harder, L. F., Hynes, M. E., Ishihara, K., Koester, J. P., Liao, S. S. C., Marcuson III, W. F., Martin, G. R., Mitchell, J. K., Moriwaki, Y., Power, M. S., Robertson, P. K., Seed, R. B. and Stokoe II, K. H. (2001). Liquefaction resistance of soils: summary report from the 1996 NCEER 14 and 1998 NCEER/NSF workshops on evaluation of liquefaction resistance of soils, Journal of Geotechnical and Geoenvironmental Engineering, ASCE 127(10), 817–833. https://doi.org/10.1061/(ASCE)1090-0241(2001)127:4(297).